Inorg. Chem. **2007**, *46*, 6164–6169

Pressure-Induced Cubic to Monoclinic Phase Transformation in Erbium Sesquioxide Er_2O_3

Qixun Guo,*,† Yusheng Zhao,† Chao Jiang,‡ Wendy L. Mao,†,¶ Zhongwu Wang,§ Jianzhong Zhang,† and Yuejian Wang†

LANSCE and MST, Los Alamos National Laboratory, Los Alamos, New Mexico 87545, CHESS, Wilson Laboratory, Cornell University, Ithaca, New York 14853, and Geological and Environmental Sciences and Photon Science, SLAC, Stanford University, Stanford, California 94305

Received January 29, 2007

Cubic Er_2O_3 was compressed in a symmetric diamond anvil cell at room temperature and studied in situ using energy-dispersive X-ray diffraction. A transition to a monoclinic phase began at 9.9 GPa and was complete at 16.3 GPa and was accompanied by a ~9% volume decrease. The monoclinic phase was stable up to at least 30 GPa and could be quenched to ambient conditions. The normalized lattice parameter compression data for both phases were fit to linear equations, and the volume compression data were fit to third-order Birch–Murnaghan equations of state. The zero-pressure isothermal bulk moduli (B_0) and the first-pressure derivatives (B_0') for the cubic and monoclinic phases were 200(6) GPa and 8.4 and also 202(2) GPa and 1.0, respectively. Ab initio density functional theory calculations were performed to determine optimized lattice parameters and atom positions for the cubic, monoclinic, and hexagonal phases of Er_2O_3. The calculated X-ray spectra and predicted transition pressure are in good qualitative agreement with the experimental results.

Introduction

Phase transformations in rare-earth sesquioxides (RE_2O_3) have been the subject of a large number of solid-state structural studies.[1−8] Goldschmidt et al. first investigated the rare-earth sesquioxides systematically in 1925,[9] and their original designations for the three phases (A, B, and C) are still in use today. The C type is cubic and has space group $Ia\bar{3}$ (No. 206) and 16 formula units per unit cell. For rare-earth elements heavier than terbium (Tb), the C-type RE_2O_3 is the most stable form over a wide temperature range at ambient pressure. The B type is monoclinic and has space group $C2/m$ (No. 12) and six formula units per unit cell; the A type is hexagonal and has space group $P\bar{3}m1$ (No. 164) and one formula unit per unit cell. These three phases are generally stable at temperatures below 2000 °C, with new phases designated as H or X being formed at temperatures above 2000 °C.[10]

Previous studies indicate that the C to B transition temperature increases with a decrease of the ionic radius of the rare-earth cation.[11] Erbium (Er) has a small ionic radius, so its extrapolated transformation temperature at ambient pressure should be high and may exceed its melting point (~2400 °C). The density of the B type is generally much higher than that of the C type ($\rho_B > \rho_C$), so the transition temperature should be reduced at high pressure.[1,2,12] Hoekatra

* To whom correspondence should be addressed. E-mail: qxguo@lanl.gov (temporary), guoqixun@ustc.edu (permanent).
† LANSCE, Los Alamos National Laboratory.
‡ MST, Los Alamos National Laboratory.
§ Cornell University.
¶ Stanford University.

(1) Hoekstra, H. R.; Gingerich, K. A. *Science* **1964**, *146*, 1163−1164.
(2) Hoekstra, H. R. *Inorg. Chem.* **1966**, *5*, 754−757.
(3) Atou, T.; Kusaba, K.; Fukuoka, K.; Kikuchi, M.; Syono, Y. *J. Solid State Chem.* **1990**, *89*, 378−384.
(4) Chen, G.; Peterson, J. R.; Brister, K. E. *J. Solid State Chem.* **1994**, *111*, 437−439.
(5) Meyer, C.; Sanchez, J. P.; Thomasson, J.; Itie, J. P. *Phys. Rev. B* **1995**, *51*, 12187−12193.
(6) Kim, Y. J.; Kriven, W. M. *J. Mater. Res.* **1998**, *13*, 2920−2931.
(7) Tang, M.; Lu, P.; Valdez, J. A.; Sickafus, K. E. *J. Appl. Phys.* **2006**, *99*, 063514-1−063514-7.
(8) Dilawar, N.; Varandani, D.; Pandey, V. P.; Kumar, M.; Shivaprasad, S. M.; Sharma, P. K.; Bandyopadhyay, A. K. *J. Nanosci. Nanotechnol.* **2006**, *6*, 105−113.
(9) Goldschmidt, V. M.; Ulrich, F.; Barth, T. *Skr. Nor. Vidensk.−Akad. Oslo, I: Nat. Naturv. Kl. No. 5* **1925**.
(10) Adachi, G. Y.; Imanaka, N. *Chem. Rev.* **1998**, *98*, 1479−1514.
(11) Warshaw, I.; Roy, R. *J. Phys. Chem.* **1961**, *65*, 2048−2051.
(12) Sawyer, J. O.; Hyde, B. G.; Eyring, L. *Inorg. Chem.* **1965**, *4*, 426−427.

10.1021/ic070154g CCC: $37.00
Published on Web 06/27/2007

Table 1. Optimized Lattice Parameters and Atom Positions for Cubic, Monoclinic, and Hexagonal Er_2O_3[a]

phase	lattice param	sites	*x*	*y*	*z*
cubic SG: #206 at 0 GPa	$a = b = c = 10.55$ Å, $\alpha = \beta = \gamma = 90°$, $V/Z = 73.39$ Å^3 ($Z = 16$)	Er1 (8b)	$^1/_4$	$^1/_4$	$^1/_4$
		Er2 (24d)	0.467	0	$^1/_4$
		O1 (48e)	0.391	0.152	0.380
monoclinic SG: #12 at 0 GPa	$a = 13.92$ Å, $b = 3.46$ Å, $c = 8.56$ Å, $\alpha = \gamma = 90°$, $\beta = 100.36°$, $V/Z = 67.59$ Å^3 ($Z = 6$)	Er1 (4i)	0.135	$^1/_2$	0.488
		Er2 (4i)	0.191	$^1/_2$	0.137
		Er3 (4i)	0.468	$^1/_2$	0.186
		O1 (4i)	0.128	0	0.282
		O2 (4i)	0.326	$^1/_2$	0.031
		O3 (4i)	0.294	$^1/_2$	0.377
		O4 (4i)	0.471	0	0.343
		O5 (2b)	0	$^1/_2$	0
monoclinic SG: #12 at 31 GPa	$a = 12.63$ Å, $b = 3.40$ Å, $c = 8.14$ Å, $\alpha = \gamma = 90°$, $\beta = 97.97°$, $V/Z = 57.70$ Å^3 ($Z = 6$)	Er1 (4i)	0.138	$^1/_2$	0.490
		Er2 (4i)	0.185	$^1/_2$	0.137
		Er3 (4i)	0.462	$^1/_2$	0.194
		O1 (4i)	0.136	0	0.297
		O2 (4i)	0.326	$^1/_2$	0.022
		O3 (4i)	0.307	$^1/_2$	0.357
		O4 (4i)	0.479	0	0.346
		O5 (2b)	0	$^1/_2$	0
hexagonal SG: #164 at 0 GPa	$a = b = 3.64$ Å, $c = 5.84$ Å, $\alpha = \beta = 90°$, $\gamma = 120°$, $V/Z = 67.01$ Å^3 ($Z = 1$)	Er1 (2d)	$^1/_3$	$^2/_3$	0.250
		O1 (2d)	$^1/_3$	$^2/_3$	0.646
		O2 (1a)	0	0	0

[a] Reported lattice parameters of the monoclinic phase at ambient conditions by Hoekstra et al.:[1,2] $a = 13.87$ Å, $b = 3.47$ Å, $c = 8.555$ Å, $\alpha = \gamma = 90°$, $\beta = 100.17°$, and $V/Z = 67.55$ Å^3. Extracted lattice parameters of the monoclinic phase at ambient conditions from our current experiment: $a = 13.866$ Å, $b = 3.473$ Å, $c = 8.579$ Å, $\alpha = \gamma = 90°$, $\beta = 100.04°$, and $V/Z = 67.802$ Å^3.

et al. investigated polymorphism in rare-earth sesquioxides at high temperature (~1000 °C) and pressure (several gigapascals). They synthesized the B type of the previously unknown heavy rare-earth sesquioxide Er_2O_3 in a large-volume press (LVP) and successfully quenched this phase back to ambient conditions.[1,2]

Here we first present an experimental and theoretical study on the pressure-induced C- to B-type phase transformation in Er_2O_3 at room temperature. Energy-dispersive X-ray diffraction was carried out in situ at high pressure and ambient temperature in a symmetric diamond anvil cell. Ab initio density functional theory (DFT) calculations were performed to obtain theoretical data for comparison with the experimental results.

Experimental Section

The submicron-sized Er_2O_3 sample was purchased from Acros and was identified as having a cubic structure using X-ray diffraction at ambient conditions. The powder sample was loaded into a ~200-μm-diameter hole drilled through a stainless steel gasket along with a ruby grain for pressure calibration,[13] and silicon oil was added as a pressure-transmitting medium. Diamond anvils with ~350 μm culets were used to compress the sample. The X-ray beam size was focused to ~10 μm. Energy-dispersive X-ray diffraction patterns were collected with a fixed 2θ (~15°) on the bending magnet beam line (B1 station) at the Cornell High Energy Synchrotron Source (CHESS), Cornell University. The radiation sources ^{55}Fe and ^{133}Ba were used for the energy calibration. Five peaks from the gold standard were used for the angle calibration. There was no overlap of Er fluorescence lines ($K\alpha_1$ at ~48 keV and $K\alpha_2$ at ~49 keV) because the measured energy range was from 10 to 35 keV, which corresponds to a *d*-spacing range of ~4.74 to ~1.35 Å.

Ab initio DFT calculations were performed to obtain optimized lattice parameters and atom positions for the C, B, and A phases of Er_2O_3 and to predict the C- to B-type transition pressure at $T = 0$ K. We employed the all-electron Blöchl's projector augmented wave (PAW) approach[14] within the generalized gradient approximation, as implemented in the Vienna ab initio simulation package (VASP).[15] The plane-wave cutoff energy was set at 500 eV. The *k*-point meshes for Brillouin zone sampling were constructed using the Monkhorst−Pack scheme.[16] We used $6 \times 6 \times 6$, $4 \times 14 \times 6$, and $15 \times 15 \times 9$ *k*-point meshes for the cubic (80-atom), monoclinic (30-atom), and hexagonal (5-atom) unit cells of Er_2O_3, respectively. Such parameters were found to be sufficient to give fully converging results.

Results and Discussion

Table 1 shows the optimized lattice parameters and atom positions for C, B, and A phases of Er_2O_3 calculated by using ab initio DFT. Among them, the atom positions for the B and A phases and the lattice parameters for the A phase were reported for the first time. Our theoretical lattice parameters and the atom positions for C and B phases are in good agreement with those of the previous reports.[10,17] From these theoretical data, simulated X-ray diffraction patterns were obtained using *PowderCell for Windows*[18] (Figure 1).

(13) Mao, H. K.; Xu, J. A.; Bell, P. M. *J. Geophys. Res.* **1986**, *191*, 4673−4676.

(14) Kresse, G.; Joubert, D. *Phys. Rev. B* **1999**, *59*, 1758−1775.

(15) Kresse, G.; Furthmuller, J. *Phys. Rev. B* **1996**, *54*, 11169−11186.

(16) Monkhorst, H. J.; Pack, J. D. *Phys. Rev. B* **1976**, *13*, 5188−5192.

(17) Hirosaki, N.; Ogata, S.; Kocer, C. *J. Alloys Compd.* **2003**, *351*, 31−34.

(18) Kraus, W.; Nolze, G. *PowderCell for Windows*, version 1.0; Federal Institute for Materials Research and Testing: Berlin, Germany, 1997.

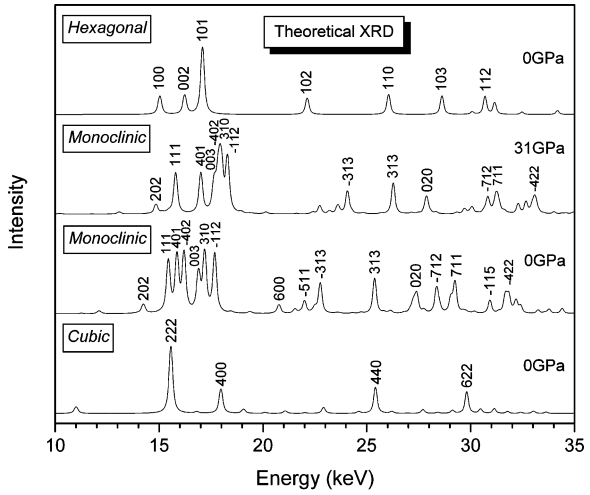

Figure 1. Simulated X-ray diffraction patterns for cubic, monoclinic, and hexagonal Er_2O_3.

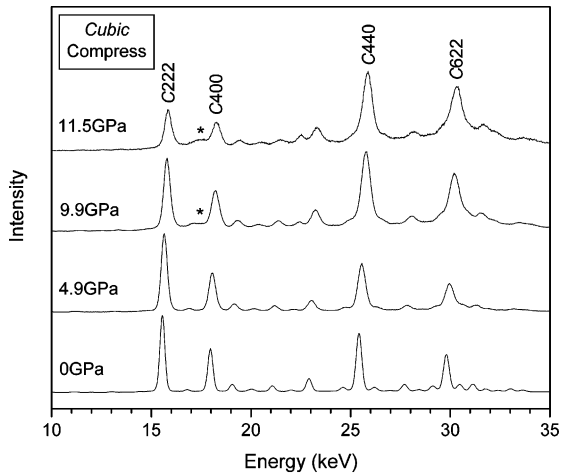

Figure 2. Representative X-ray diffraction patterns for cubic Er_2O_3 up to 11.5 GPa.

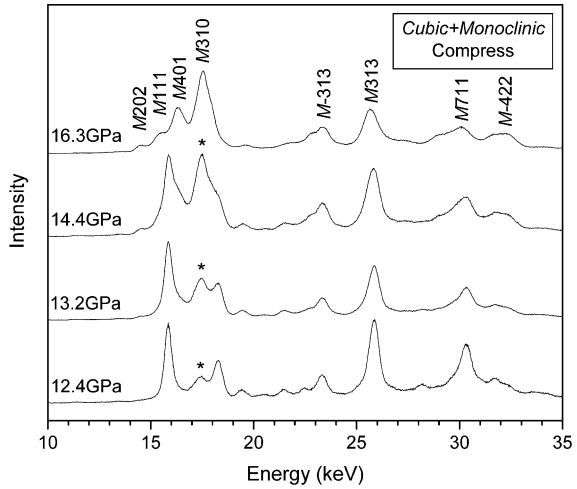

Figure 3. Representative X-ray diffraction patterns for a mixture of cubic and monoclinic Er_2O_3 up to 16.3 GPa.

Figures 2 and 3 show representative X-ray diffraction patterns for cubic Er_2O_3 up to 11.5 GPa and a mixture of cubic and monoclinic Er_2O_3 up to 16.3 GPa, respectively. All diffraction peaks in Figure 2 can be well-indexed to cubic Er_2O_3. Fitting the peaks of the starting sample at ambient

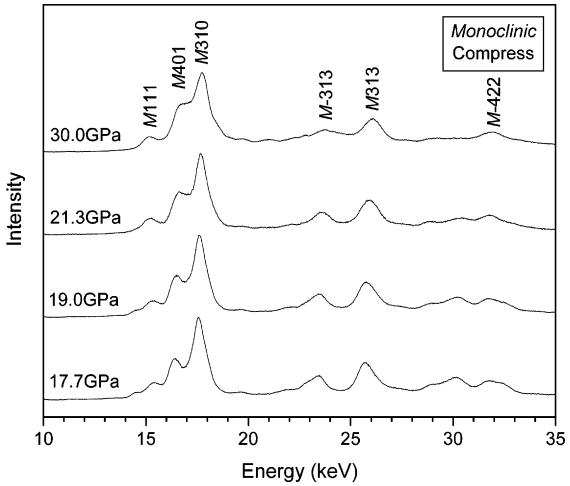

Figure 4. Representative X-ray diffraction patterns for monoclinic Er_2O_3 up to 30 GPa.

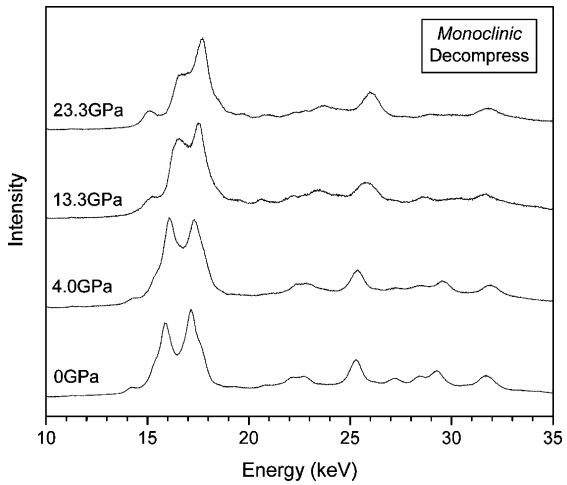

Figure 5. Representative X-ray diffraction patterns of Er_2O_3 decompressed to ambient conditions.

pressure (0.1 MPa ≅ 0 GPa) to a cubic structure gave a_0 = 10.5536(40) Å (V/Z = 73.465 Å^3 and Z = 16), which is in good agreement with the reported value of a_0 = 10.53 Å (JCPDS No. 77-0777) and the theoretically calculated value of a_0 = 10.55 Å (Table 1) for C-type Er_2O_3. Between 9.9 and 11.5 GPa, the relative intensity of the C222 peak became increasingly weak, indicating a change in the atomic positions in cubic Er_2O_3. At the same time, new broad peaks marked with asterisks began to appear between C222 and C400. By 16.3 GPa, the peaks of C-type Er_2O_3 had completely disappeared and the sample was fully converted to the B type. No further discontinuous changes were observed in the X-ray diffraction patterns (Figure 4) with increasing pressure up to 30 GPa. After the pressure was released, the B-type Er_2O_3 could be quenched to ambient conditions (Figure 5).

Using the simulated X-ray diffraction patterns for Er_2O_3 (see Figure 1) as references, the high-pressure phase can be indexed as a monoclinic cell (B type). Figure 6 shows a comparison of the experimental and theoretical X-ray diffraction patterns for the monoclinic phase at ambient pressure. The lattice parameters calculated from the experimental spectra are as follows: a = 13.866(33) Å, b = 3.473(16) Å, c = 8.579(20) Å, $\alpha = \gamma = 90°$, β = 100.04(12)°,

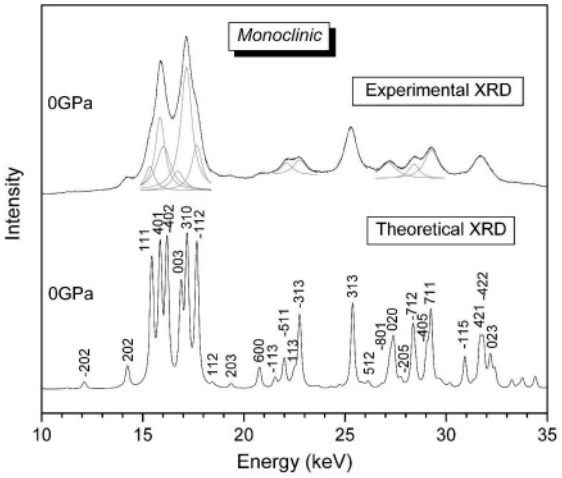

Figure 6. Comparison of the experimental and theoretical X-ray diffraction patterns of the monoclinic phase.

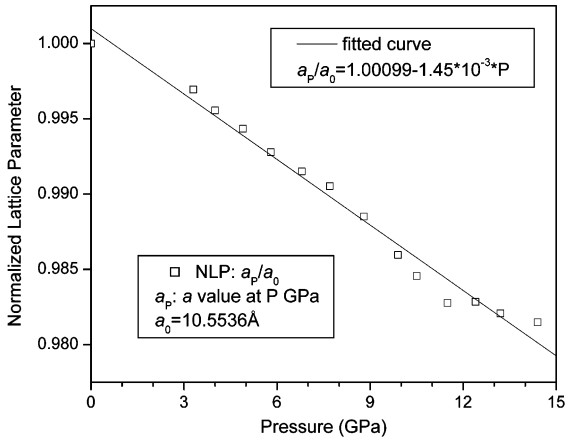

Figure 7. Room-temperature NLP−volume data for cubic Er_2O_3 upon compression.

and $V/Z = 67.802$ Å^3 ($Z = 6$), which are in good agreement with our theoretical results and previous reports (see Table 1). The shape of the X-ray diffraction patterns of Er_2O_3 at 17.7 GPa is very similar to the reported B-type Yb_2O_3 at 18 GPa and room temperature,[5] which also supports the formation of B-type Er_2O_3 in our experiments.

The full-width at half-maximum (fwhm) of the C440 peak at 0.1 MPa is 0.2757 keV. When the pressure was increased to 4.9 GPa, a broadening of the C440 peak was observed and the fwhm reached 0.3725 keV (an increase of 35%). At 30 GPa, the fwhm of the B313 peak was 0.7206 keV (an increase of 161%). This broadening, while significant, did not affect the phase analysis and determination. It should also be noted that none of the X-ray diffraction patterns (at any pressure) in our experiment could be indexed as the A-type hexagonal phase, indicating that Er_2O_3 does not transform into the A type from the C type at room temperature below 30 GPa.

Extrapolation of the previously reported high-temperature data to room temperature[2] would give a predicted transition pressure for C- to B-type Er_2O_3 of ∼5 GPa. Ab initio DFT calculations give a theoretical transition pressure of ∼7 GPa. Our experimental value (∼9.9 GPa) is slightly higher than

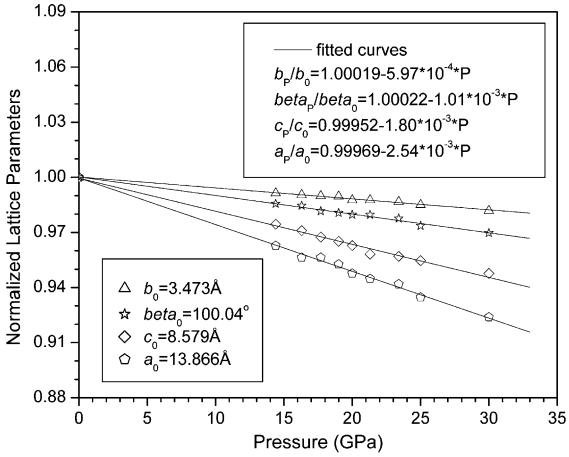

Figure 8. Room-temperature NLP−volume data for the monoclinic Er_2O_3 upon compression.

both the high-temperature extrapolation and the theoretical value but is in good qualitative agreement.

Figures 7 and 8 show room-temperature normalized lattice parameter (NLP)−volume data for cubic and monoclinic Er_2O_3, respectively. The NLP compression for both phases was fit to linear equations (1)−(5).

For the cubic phase:

$$a_P/a_0 = 1.00099 - 1.45 \times 10^{-3}P, \quad a_0 = 10.5536\ \text{Å} \tag{1}$$

For the monoclinic phase:

$$a_P/a_0 = 0.99969 - 2.54 \times 10^{-3}P, \quad a_0 = 13.866\ \text{Å} \tag{2}$$

$$b_P/b_0 = 1.00019 - 5.97 \times 10^{-4}P, \quad b_0 = 3.473\ \text{Å} \tag{3}$$

$$c_P/c_0 = 0.99952 - 1.80 \times 10^{-3}P, \quad c_0 = 8.579\ \text{Å} \tag{4}$$

$$\beta_P/\beta_0 = 1.00022 - 1.01 \times 10^{-3}P, \quad \beta_0 = 100.04° \tag{5}$$

The axial compression sequence was found to be correlated to the axial length sequence in the monoclinic phase of Er_2O_3. The compressibilities along the *a* and *c* axes in the monoclinic phase and along the *a* axis in the cubic phase have the same order of magnitude. In contrast, the compressibility along the *b* axis in the monoclinic phase is about an order of magnitude smaller. The above results indicate that the *a* and *c* axes are more compressible than the *b* axis. This semiempirical law has been applied to a number of cases[4,5] and also holds true here.

Figure 9 shows the room-temperature pressure−volume data for Er_2O_3 upon compression and decompression. The data for the cubic and monoclinic phases were fit to the Birch−Murnaghan equation of state (6).[19,20]

$$P(V) = \frac{3B_0}{2}\left[\left(\frac{V_0}{V}\right)^{7/3} - \left(\frac{V_0}{V}\right)^{5/3}\right]\left\{1 + \frac{3}{4}(B_0' - 4)\left[\left(\frac{V_0}{V}\right)^{2/3} - 1\right]\right\} \tag{6}$$

The zero-pressure isothermal bulk moduli B_0 and the first-pressure derivatives B_0' for cubic and monoclinic phases were 200(6) GPa and 8.4 and also 202(2) GPa and 1.0, respectively. The phase transformation was accompanied by a ∼9%

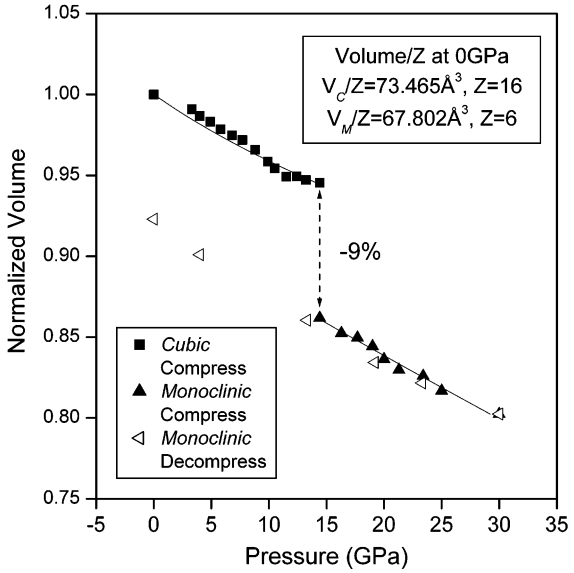

Figure 9. Room-temperature pressure-volume data for Er_2O_3 upon compression and decompression.

volume decrease. From the pressure−volume data for monoclinic Er_2O_3 upon compression and decompression, one can see that, at the same pressure, the volume at the compression stage is a little smaller than that at the decompression stage. This kind of hysteresis effect is fairly common and has been observed in many solid-state reactions.[21]

While the C- and B-type forms of Er_2O_3 have been observed experimentally, three other forms (the A, H, and X types) have been predicted but have not yet been detected in experiments. The phase transformation from the C to B type is reconstructive, and the B type could be quenched to ambient conditions. Quenching of the B type was also observed by Hoekstra et al.[1] after synthesis in a LVP at 3 GPa and 1020 °C. Herein, we further evidence that B-type Er_2O_3 can be retained at room temperature by pressure quenching to ambient pressure. It should be noted that B-type (high-pressure phase) Er_2O_3 is not thermodynamically stable at atmospheric pressure and below 2000 °C. It would eventually revert to the C type (low-pressure phase), but the transformation speed is exceedingly sluggish because of the high kinetic barrier related to crystal reconstruction. Previous experiments indicate that the transformation from the B type back to the C type can be realized by annealing the B type in air at atmospheric pressure and 900 °C for several hours.[2]

The phase transformation from the B to A type is displacive. It can be expected that this transition may have a smaller energy barrier because the hexagonal phase involves only a slight deformation of the monoclinic structure. The B- to A-type transition has proven difficult for researchers to observe experimentally. Previous reports on the temperature stability relationships of the rare-earth sesquioxide polymorphs[11] indicate that, at ambient pressure, the phase boundary between the B and A types (for light rare-earth atoms Nd through Sm) is almost vertical and virtually independent of temperature, making it is hard to observe this phase transformation by the application of high temperature alone.[2] Atou et al. reported a reversible B- to A-type transition of Sm_2O_3 under high pressure using in situ X-ray diffraction,[22] and so far this is the only report of B- to A-type phase transformation in the lanthanide sesquioxides (Ln_2O_3).

The C- to B-type transformation occurs with a substantial density increase. In contrast, the transformation from the B to A type results in a minor density decrease. The theoretical density for B-type Er_2O_3 at ambient conditions is 9.401 g·cm^{-3}, which is very close to our experimental value of 9.371 g·cm^{-3} and previously reported value of 9.406 g·cm^{-3}. In contrast, the theoretical density of the A type at ambient conditions is 9.482 g·cm^{-3}. The relative theoretical density difference of the two phases at ambient conditions is only 0.86%. At high pressures, this difference is expected to become even smaller (approaching zero), which would further reduce the $P\Delta V$ term for driving the phase transformation.

The Gibbs free-energy change due to a phase transition is given by[20,23]

$$\Delta G(P,T) = \Delta^\circ H(T) - T\Delta^\circ S(T) + \int_0^p \Delta V(P,T)\,\mathrm{d}P \qquad (7)$$

At equilibrium, $\Delta G(P,T) = 0$. Assuming that both phases have the same compressibility and thermal expansion and that the phase transition has no effect on the heat capacity, a simplified equation can be obtained and used to calculate the transition pressure as a function of the temperature:

$$P_{tr} = (\Delta H^\circ - T\Delta^\circ S)/(-\Delta V) \qquad (8)$$

At room temperature, $T = 300$ K, $\Delta^\circ H$ is typically 1 order of magnitude larger than $T\Delta^\circ S$ in lanthanide sesquioxides. Thus, eq 8 may be further simplified as

$$\Delta^\circ H \approx P_{tr}(-\Delta V) \qquad (9)$$

If we know the transition pressure and volume change in a phase transition in lanthanide sesquioxides at room temperature, we may estimate the enthalpy change.

In our current work, the theoretical enthalpy change for the cubic to monoclinic phase transformation may be estimated as follows:

$$\Delta^\circ H \approx P_{tr}(-\Delta V) = 7\ \mathrm{GPa} \times 5.8\ \text{Å}^3 \times 6.02 \times 10^{23}/\mathrm{mol} = 24\ \mathrm{kJ \cdot mol^{-1}}$$

The above estimated enthalpy change is in qualitative

(19) Anderson, O. L. *Equations of State of Solids for Geophysics and Ceramic Science*; Oxford University Press: New York, 1995.
(20) Hemley, R. J. *Ultrahigh-Pressure Mineralogy: Physics and Chemistry of the Earth's Deep Interior*; Mineralogical Society of America: Washington, DC, 1998.
(21) Flanagan, T. B.; Park, C. N.; Oates, W. A. *Prog. Solid State Chem.* **1995**, *23*, 291−363.
(22) Atou, T.; Kusaba, K.; Tsuchida, Y.; Utsumi, W.; Yagi, T.; Syono, Y. *Mater. Res. Bull.* **1989**, *24*, 1171−1176.
(23) Matvei, Z. *Prog. Mater. Sci.* **2007**, *52*, 597−647.

agreement with the reported data for some C- to B-type phase transformations in Ln_2O_3.[23]

Conclusions

We studied a pressure-induced cubic to monoclinic phase transformation in Er_2O_3 at room temperature by in situ synchrotron X-ray diffractions. We also performed ab initio DFT calculations to obtain theoretical data related to the three phases of Er_2O_3 and their phase transformations. The theoretical data are in good qualitative agreement with the experimental results, indicating that ab initio DFT calculations worked well for Er_2O_3. The current research would give us a new guideline to effectively investigate the phases and their transformations in lanthanide sesquioxides (Ln_2O_3) by a powerful combination of synchrotron X-ray diffractions and ab initio DFT calculations.

Acknowledgment. Both Q.G. and C.J. are supported by Director's Postdoctoral Fellowships, and W.L.M. is supported by a J. R. Oppenheimer Fellowship at Los Alamos National Laboratory (LANL). The experimental work was performed under the auspices of the LDRD-PRD program (No. 20061378) at LANL and based upon research conducted at the Cornell High Energy Synchrotron Source (CHESS), which is supported by the National Science Foundation under Award DMR-0225180. The theoretical work was performed using the computing facilities at LANL.

IC070154G